

Rongjie Zhao and Feng Zhao contributed equally to this work.

Key Points:

- A deep seamount effect upon microplankton was revealed
- Deep seamount enhanced vertical connectivity and cooccurrence complexity of ciliate community
- Ciliate communities presented a much higher-resolution record of deep seamount effects than physico-chemical data

Supporting Information:

Supporting Information may be found in the online version of this article.

Correspondence to:

K. Xu,
kxu@qdio.ac.cn

Citation:

Zhao, R., Zhao, F., Feng, L., Fang, J. K.-H., Liu, C., & Xu, K. (2023). A deep seamount effect enhanced the vertical connectivity of the planktonic community across 1,000 m above summit. *Journal of Geophysical Research: Oceans*, 128, e2022JC018898. <https://doi.org/10.1029/2022JC018898>

Received 25 MAY 2022

Accepted 18 FEB 2023

Author Contributions:

Conceptualization: Rongjie Zhao, Feng Zhao, Kuidong Xu
Data curation: Rongjie Zhao, Ling Feng, Chuanyu Liu
Formal analysis: Rongjie Zhao
Funding acquisition: Feng Zhao, Kuidong Xu
Investigation: Rongjie Zhao, Feng Zhao, Ling Feng, Chuanyu Liu
Methodology: Rongjie Zhao, Feng Zhao
Project Administration: Kuidong Xu
Resources: Kuidong Xu
Software: Rongjie Zhao, Feng Zhao
Supervision: Kuidong Xu
Validation: Rongjie Zhao, Feng Zhao
Visualization: Rongjie Zhao, Ling Feng, Chuanyu Liu
Writing – original draft: Rongjie Zhao, Feng Zhao, Ling Feng, Chuanyu Liu

A Deep Seamount Effect Enhanced the Vertical Connectivity of the Planktonic Community Across 1,000 m Above Summit

Rongjie Zhao¹ , Feng Zhao^{1,2} , Ling Feng³, James Kar-Hei Fang^{4,5} , Chuanyu Liu³ , and Kuidong Xu^{1,2,6} 

¹Laboratory of Marine Organism Taxonomy and Phylogeny, Qingdao Key Laboratory of Marine Biodiversity and Conservation, Center for Ocean Mega-Science, Institute of Oceanology, Chinese Academy of Sciences, Qingdao, China, ²Southern Marine Science and Engineering Guangdong Laboratory (Zhuhai), Zhuhai, China, ³Key Laboratory of Ocean Circulation and Waves, Institute of Oceanology, Chinese Academy of Sciences, Qingdao, China, ⁴Department of Applied Biology and Chemical Technology, The Hong Kong Polytechnic University, Hung Hom, China, ⁵State Key Laboratory of Marine Pollution, City University of Hong Kong, Kowloon Tong, China, ⁶University of Chinese Academy of Sciences, Beijing, China

Abstract Seamount effects, which are generally defined as hydrographic disturbances caused by topography and nutrient enrichment and biological aggregations around seamounts, are normally observed in shallow seamounts due to limited sampling efforts in deep seamounts. However, it remains unclear how and to what extent do deep seamounts leave their imprint on planktonic communities. Herein ciliates, a representative protist group, were chosen to explore the effect of deep seamount on planktonic community. By investigating the vertical and horizontal distribution of ciliate communities around the Kocebu Guyot (summit at −1,198 m) and in nonseamount area, we revealed an obvious deep seamount effect, which enhanced the vertical mixing of ciliate communities to an extent of over 1,000 m above the summit. The vertical mixing was manifested by a strong uplift of bottom dwellers from waters deeper than 500 m and a weak uplift from the 300 m layer to the deep chlorophyll maximum (about 150 m) layer. Network analysis showed that the ciliate cooccurrence relationship around the seamount was much more complex than that in nonseamount area. Statistical analysis indicated that seamount significantly weakened the limitation that water depth posed on vertical ciliate distribution. Overall, the ciliate communities presented a much higher-resolution record of deep seamount effects than physico-chemical data. Deep seamount could enhance the vertical mixing of waters and cooccurrence complexity of planktonic community to the euphotic layer. Considering the wide existence of deep seamounts, such an effect may have ecological significance and enhance the cycles of matter and energy of global oceans.

Plain Language Summary Seamounts are widely distributed undersea mountains. The specific topography and hydrography of seamounts directly or indirectly enrich the concentrations of particle organic matter and subsequently enhance primary production. This phenomenon is known as a seamount effect and is generally found in shallow (summit depth <200 m) and intermediate seamounts (summit depth 200–400 m). In order to find out whether and to what extent can deep seamount (summit depth >400 m) have a seamount effect on surrounding environments, we explored planktons around a deep seamount with a summit depth of about 1,200 m. We found a distinct deep seamount effect, which could enhance vertical mixing of planktons to an extent of over 1,000 m above the summit. The vertical mixing was composed of a strong uplift of benthos in waters deeper than 500 m and a weak uplift from the 300 m layer to deep chlorophyll maximum (about 150 m) layer. Such a deep seamount effect has never been documented before and may have ecological significance and enhance the cycles of matter and energy of global oceans.

1. Introduction

Seamounts are widespread undersea mountains with a height of more than 1,000 m and have been focal areas of biological diversity and biogeography research (Clark et al., 2010; Rogers, 1994; Stocks et al., 2012). It is well known that seamounts act as “hotspots” of benthos, while fish, zooplankton, and other pelagic marine lives are also found to aggregate around seamounts (Genin, 2004; Koslow et al., 2000; Rogers, 2018). At shallow (summit depth 0–200 m) and intermediate (summit depth 200–400 m) seamounts, interactions between topography and hydrography generate physical changes such as vertical mixing, internal waves, and Taylor column and

Writing – review & editing: Feng Zhao,
James Kar-Hei Fang, Kuidong Xu

subsequently enhance organic matter and inorganic nutrients in the euphotic zone above the seamounts, resulting in the promoting of primary productions (Chapman & Haidvogel, 1992; Genin, 2004; Mohn et al., 2021; Read & Pollard, 2017). A study exploring the circulation pattern around a deep seamount (summit $-1,308$ m) in the northwest Pacific Ocean found a deep anticyclonic cap enclosing the entire seamount at a depth of 728 m (Guo et al., 2020). Likewise, recent studies on the Kocebu Guyot with a summit depth of 1,198 m showed that the seamount influenced particulate organic carbon in the upper waters to up to a depth of 750 m (Ma et al., 2020a), as well as nutrients in the bottom layer of the euphotic zone, to result in high biomass of phytoplankton (Dai et al., 2022). These findings have extended our understanding of the ecological importance of deep seamounts and give clues about the deep seamount effects. A recent study of planktonic bacteria, protists, and fungi around the Kocebu Guyot gave clues about deep seamount effects, but the scope of the effect was unclear due to a lack of distinct indicators (Zhao, Zhao, Zheng, et al., 2022). Whether and to what extent do deep seamounts have any imprint on planktonic community remains unclear.

Ciliates (Alveolata, Ciliophora) are a representative, highly diverse microeukaryotic group widely distributed in world oceans (Fenchel, 1987; Foissner, 2006). They are vital components of microzooplankton in microbial food webs as bridges between primary producers and larger consumers in marine environments (Azam et al., 1983; Pierce & Turner, 1992). Numerous studies on ciliate diversity and distribution have been conducted in the open ocean areas. Close correlations between ciliates communities and phytoplankton richness as well as environmental variations were found in the Atlantic Ocean (Dolan et al., 2002) and in the polar oceans (Jiang et al., 2014). Moreover, an obvious stratification of ciliate community was detected not only in the sunlit ocean on a global scale (de Vargas et al., 2015; Gimmler et al., 2016) but also from the surface to the abyssopelagic zone in the western Pacific Ocean (Zhao, Filker, Stoeck, et al., 2017). In terms of the seamount communities, Zhao, Filker, Xu, et al. (2017) investigated benthic ciliates on a seamount and showed that water depth was a less important factor shaping the distribution of ciliates, which was distinctly different from those in shallow seafloors. This implied that the seamount might enhance the transport of ciliates along the gradient of the water depth through the passive dispersal of ocean currents. All these findings indicate that ciliates could serve as a suitable representative to uncover the effect of deep seamount on the diversity and distribution patterns of microplanktonic community.

In this study, we hypothesized that planktonic ciliates, a widely distributed protist group with broad niche widths, might provide similar imprint of deep seamount effects as indicated by physico-chemical and phytoplankton data. In order to understand the mechanism of deep seamount effects, ciliate communities in the water columns around the deep seamount Kocebu Guyot and those in a nonseamount area in the western Pacific Ocean were determined with high throughput sequencing. We aimed to study the variation in the vertical connectivity and community interactome of plankton between the deep seamount and nonseamount areas and to estimate to what extent deep seamounts could have an effect on the planktonic community.

2. Materials and Methods

2.1. Study Area and Sample Collection

The Kocebu Guyot is a flat-topped deep seamount of the Magellan Seamount Chain in the western Pacific Ocean, with a summit depth of about 1,198 m and a height of about 4,000 m. During the cruise of *R/V KeXue* in 2018, we collected a total of 38 full-depth water samples from five stations, A2, A5, A8, B1, and B8, around the Kocebu Guyot (Figure 1 and Table S1 in Supporting Information S1). The sampling stations and collection procedure had been described by Zhao, Zhao, Zheng, et al. (2022), who studied the diversity of planktonic bacteria, protists, and fungi around the seamount. Briefly, station A5 was located above the seamount, and the other four stations were situated around the seamount where water currents flowed along or perpendicular to the stations. A total of 20 L water was collected from each water layer at each station, which were then filtered first through a 200 μm sieve, then a 0.22 μm polycarbonate filter. All polycarbonate filters were immediately put in liquid nitrogen and stored at -80°C until laboratory processing.

For comparison with nonseamount area, data from three stations of the Philippine Basin in the western Pacific Ocean (Figure 1 and Table S2 in Supporting Information S1) were downloaded from National Center for Biotechnology Information (NCBI) under the accession number SRP139064 (Zhao, Filker, Stoeck, et al., 2017).

Water temperature, salinity, and sampling depth were measured in situ via a CTD probe. Dissolved oxygen (DO) was measured in situ by Winkler iodometry at $\leq 2\%$ relative standard deviation after fixation with manganese

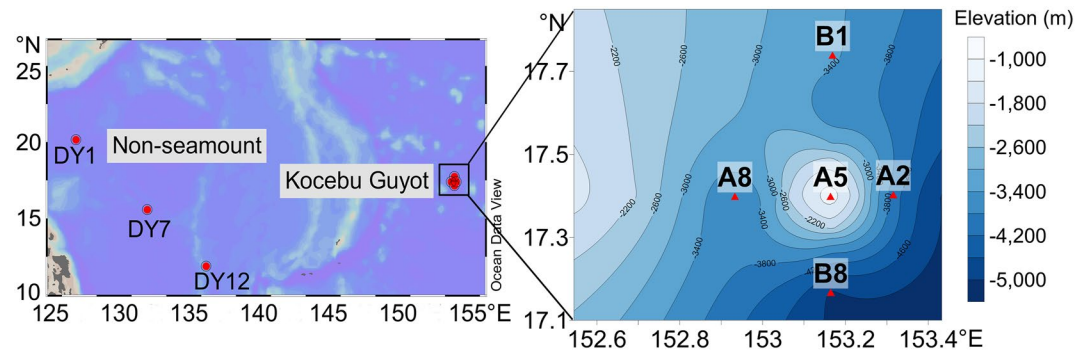


Figure 1. Sampling stations in the Kocebu Guyot and nonseamount areas. A5 is located at the summit of the Kocebu Guyot and the other four stations are situated around the seamount.

sulfate and alkaline potassium iodide solution (Ma et al., 2020b). Chlorophyll *a* (Chl *a*) was extracted in 90% acetone at 4°C for 24 hr and measured using a Turner Designs Trilogy Fluorometer (Turner Designs, USA; Parsons et al., 1984). The concentrations of NO₃-N, NO₂-N, PO₄-P, SiO₃-Si, and NH₄-N of water samples were determined with a continuous flow analyzer (QuAatro, Seal Analytical Limited, UK) according to the Joint Global Ocean Flux Study (JGOFS) spectrophotometric method (Gordon et al., 1993) after filtration through borosilicate glass microfiber filters (Whatman Grade GF/F filter). Concentrations of total nitrogen (TN) and total phosphorus (TP) in seawater were quantified with a continuous flow analyzer (QuAatro, Seal Analytical Limited, UK) after persulfate oxidation. The concentrations of Chl *a*, DO, NO₃-N, NO₂-N, PO₄-P, SiO₃-Si, and NH₄-N of seamount samples were integrated in Table S3 in Supporting Information S1. The concentrations of Chl *a*, NO₃-N, NO₂-N, PO₄-P, SiO₃-Si, NH₄-N, TN, and TP of nonseamount samples were integrated in Table S4 in Supporting Information S1.

To describe the physical drivers and mechanisms responsible for the biological distributions observed, the delay time altimetry product provided by Archiving Validation and Interpretation of Satellite Oceanographic data (AVISO) Version 3 was used here. This multiple-satellite-merged data set contains global gridded sea level anomaly and sea surface geostrophic current anomaly data with a 1/4° resolution from January 1993 to December 2020, which can provide information of mesoscale eddies in the study area. The data are available at www.avisio.altimetry.fr. In addition, a 3-day averaged output from an eddy-permitting reanalysis model ECCO2 based on MITgcm was applied to obtain the vertical velocity around the Kocebu Guyot and the nonseamount area. Here, ECCO2 is abbreviation for the “Estimating the Circulation and Climate of the Ocean” synthesis version 2 (Menemenlis et al., 2008), and MITgcm for the Massachusetts Institute of Technology General Circulation Model (Marshall et al., 1997). The horizontal resolution of ECCO2 is 1/4°, and the time ranges from 2009 to 2013. There are 50 uneven vertical levels, with the thicknesses ranging from about 10 m in the upper 150 m to about 400 m below 5,000 m. The ECCO2 data are available at <http://apdr.c.soest.hawaii.edu/las/v6/dataset?catitem=4837>.

2.2. Laboratory Procedure and DNA Sequencing

Environmental DNA of seamount samples was extracted using All Prep DNA/RNA Mini Kit (Qiagen, Germany) following the manufacturer’s instructions. The 18S rRNA V4 region of ciliate was amplified using a nested PCR approach (Stock et al., 2013) with two sets of primers. First, CiliF and CiliR I–III (Lara et al., 2007) were used to amplify the 18S rRNA gene of ciliates; second, the purified PCR product was used to amplify the hypervariable V4 region of ciliate 18S rRNA with primers Reuk454FWD1 and TAREukREV3 (Stoeck et al., 2010).

Subsequently, the final PCR products were sequenced using the Illumina MiSeq platform (Illumina, Inc., San Diego, CA). The merged clean reads were submitted to downstream analysis. DNA sequences of nonseamount samples were generated using the same method by Zhao, Filker, Stoeck, et al. (2017).

2.3. Data Processing and Statistical Analysis

2.3.1. Generating Zero-Radius Operational Taxonomic Units Table

The obtained seamount data combining with nonseamount data were dereplicated and singletons were excluded using USEARCH (v.11.0; Edgar, 2013). Unoise3 was used to generate zero-radius operational taxonomic unit

(ZOTU) of 100% similarity and the resulting ZOTUs were taxonomically assigned according to PR² (v.4.14) database using BLAST (Edgar, 2018; Edgar & Flyvbjerg, 2015; Guillou et al., 2013). Considering that not all the rarefaction curves of samples were saturated (Figure S1 in Supporting Information S1), all samples were rarefied with the minimum sample size (1,783) to ensure intersample comparability. A ZOTU table of 1,625 ciliate ZOTUs and 97,309 reads was obtained.

2.3.2. Taxonomic Diversity and Phylogenetic Diversity

We selected ZOTU richness as taxonomic alpha diversity (hereafter TDA α) and calculated it using the vegan package (Dixon, 2003). Phylogenetic diversification across regional and continental scales over a long time results in community biodiversity (Graham & Fine, 2008). The combining of phylogenetic diversity with geographic structure and environmental gradients could enable us to understand the ecological mechanisms of biodiversity (Cavender-Bares et al., 2009; Heino & Tolonen, 2017). To calculate the phylogenetic alpha diversity (hereafter PDA α) of the seamount and nonseamount samples, a phylogenetic tree was generated using aligned representative sequences of ciliate ZOTUs that were extracted from the seamount and nonseamount data sets. The representative sequences were aligned in SeaView (v.5) with MUSCLE mode (Gouy et al., 2010), then the aligned sequences were used to make the phylogenetic tree in FastTree with -gr option (Price et al., 2010). Finally, the Faith's phylogenetic diversity (i.e., the minimum total length of all the phylogenetic branches required to span a given set of taxa on the phylogenetic tree) as PDA α was calculated using the tree file and ZOTU abundance file with "pd" function in the picante package (Faith, 1992; Kembel et al., 2010). Taxonomic beta diversities (hereafter TDB β) and phylogenetic beta diversities (hereafter PDB β) were computed using "beta" function in the BAT package (Cardoso et al., 2015). We further implemented boxplot to present the TDA α and PDA α of ciliate communities in the seamount and nonseamount areas using the ggplot2 package (Wickham, 2016).

In order to evaluate the difference between seamount and nonseamount ciliate communities, we applied hierarchical cluster analysis based on Bray-Curtis distances of all samples using PRIMER (v.6). The Bray-Curtis distances were calculated using log-transformed ZOTU table. SIMPROF analysis with 999 permutations was utilized to disentangle the significant difference in similarity between samples.

2.3.3. Disentangling the Relative Importance of Deterministic and Stochastic Processes

The relative importance of ecological processes was disentangled by using β -Nearest Taxon Index (β NTI) and occurrence-based Raup-Crick matrix (β_{RC} ; Chase et al., 2011; Stegen et al., 2013, 2015). Statistical analyses were implemented with the Picante and Vegan packages (Dixon, 2003; Kembel et al., 2010).

2.3.4. Sample-Sample and Taxon-Taxon Cooccurrence Networks

In order to evaluate the cooccurrence relationships of samples, we performed the network analysis and calculated Spearman's correlation using "corr.test" function in the Psych package. With the aim to reflect robust core interactions, ZOTUs that featured (a) presence in at least four stations for nonseamount samples and seven stations for seamount samples, (b) correlations with Spearman's rank correlation coefficient >0.5 or <-0.5 , and (c) statistical significance ($P < 0.05$, all P -values were adjusted by the Benjamini and Hochberg FDR controlling procedures) were selected (Barberan et al., 2012).

Taxon-taxon cooccurrence networks of ciliate community under 1,000 m were constructed to explore the seamount effects on relationships among the ciliate taxa. To ensure interhabitat comparability, the water layers of 1,000, 2,000 m, and the bottom were sampled both from the seamount and nonseamount areas. In addition, we implemented the taxon-taxon cooccurrence network of each station from the seamount and nonseamount areas to compare the complexity of each network throughout the water column in different habitats. Taxon-taxon cooccurrence network of each water layer in the seamount was also implemented to distinguish the core taxa in different water layers. In order to highlight the core relationships, ZOTUs with an occurrence ratio of at least 50% were selected. The Spearman's correlation was calculated and any correlations with coefficient absolute value >0.6 and statistical significance ($P < 0.05$) were retained. Core taxa was defined as the taxa with the top three number of correlations.

The analysis was implemented with the igraph and pschyc packages in R and the networks were illustrated using Gephi (v.0.9.2; Mathieu et al., 2009). The size of node represented the level of interactions with other nodes, the width of line represented the absolute coefficient value of each correlation.

2.3.5. SourceTracker for Karyorelictea in Water Column Around Seamount

In order to identify the sources of benthic Karyorelictea in water column at the seamount area, SourceTracker analysis was utilized following the method of Knights et al. (2011). We sorted the samples found with Karyorelictea into different groups according to water layers and estimated the source proportions of individual water layers.

2.3.6. Evaluating the Effects of Environmental Factors on Ciliate Communities

In order to evaluate the direct and indirect effects of specific environmental factors on TDA α and PDA α of ciliate communities in the seamount and nonseamount areas, partial least squares path modeling (PLS-PM) was implemented using the PLSPM package (Sanchez, 2013a). We divided the environmental factors into four blocks (latent variables), DEPTH (sampling depth), ENV (temperature, salinity, and DO), NUTR (concentration of NO₃-N, NO₂-N, NH₄-N, PO₄-P, and SiO₃-Si) and BIO (concentration of Chl *a*), an arrangement that was enlightened by Gao et al. (2019). Due to cruise discrepancy in the nonseamount area, the ENV block only consisted of temperature and salinity, while the NUTR block included concentration of NO₃-N, NO₂-N, NH₄-N, PO₄-P, SiO₃-Si, TN, and TP. After initial permutation, factors with loading <0.7 in the outer model section were excluded and a final PLS-PM was carried out (Sanchez, 2013b).

Further analysis of environmental factors influencing the ciliate community structure was verified by the variation partitioning analysis (VPA) using the “varpart” function of the vegan package. TDBeta and PDBeta matrices of ciliate communities in seamount and nonseamount areas were used as data sets and the decomposition was based on distance-based redundancy analysis (McArdle & Anderson, 2001). The environmental factors were divided into four sections as in PLS-PM. ANOVA tests were performed on the individual variations explained by each section with 999 permutations. In order to evaluate the impact of depth upon ciliate communities in seamount and nonseamount areas, the proportion of adjusted R^2 of depth out of all factors was calculated, respectively. All statistical analyses mentioned above were conducted in R (v.3.6.2).

3. Results

3.1. Diversity and Community of Ciliates in Seamount and Nonseamount Areas

The ciliate communities in the seamount and nonseamount areas exhibited similar patterns of vertical distribution. Overall, the ciliate samples tended to group according to depth rather than sampling regions, with distinction between photic and aphotic samples. The samples in the nonseamount area were separated distinctly from the seamount samples within the photic and aphotic zones (Figure 2a). The seamount ciliate community from the 200 m layer had higher similarity with that from the photic water layers, while in the nonseamount area the ciliate community from the 200 m layer was more similar to that from the aphotic deepwater layers.

The TDA α of ciliate community exhibited an indistinctly unimodal pattern, while no clear pattern was shown for the PDA α in the seamount area, where both the TDA α and PDA α peaked in the 200 m water layer (Figure 2b). In contrast, both the TDA α and PDA α showed a distinctly unimodal distribution in the nonseamount area, where the peak values occurred in the deep chlorophyll maximum (DCM, about 150 m depth) layer, and then the diversity decreased with increasing depth.

The class Karyorelictea, as typical bottom dwellers, was unexpectedly frequent and abundant in the seamount water samples and contributed to about 44.3% of the total sequences in the water layers below 300 m (Figure S2 in Supporting Information S1). Karyorelictea sequences occurred also in the 200 m and DCM layers around the seamount, with an average proportion of 0.88%. In the nonseamount area, Karyorelictea was detected only in the 1,000 and 2,000 m layers, with an average sequence proportion of merely 0.1% (Figure 3a). Due to the presence of Karyorelictea, the sequence proportion of the class Spirotrichea out of all sequences decreased in the seamount area (52.2%) than the nonseamount area (65.15%; Figure S2 in Supporting Information S1).

The SourceTracker analysis showed that the population of Karyorelictea in the DCM was mainly derived from the lower water layers (Figure 3b), with about 28% of the sequences came from the 1,000 m layer, 24% from the 200 m layer, and 16% from the 300 m layer. As regards Karyorelictea in the 200 m layer, 32% came from the 300 m layer, 15% from the DCM, 11% from the 3,000 m layer, and 23% from unknown sources. For karyorelicteans in the 300 m layer, nearly half were derived from unknown sources, 29% from the water layers below 300 m, and about 16% from the DCM. From the 2,000 m water layer, the contribution of karyorelicteans from deeper

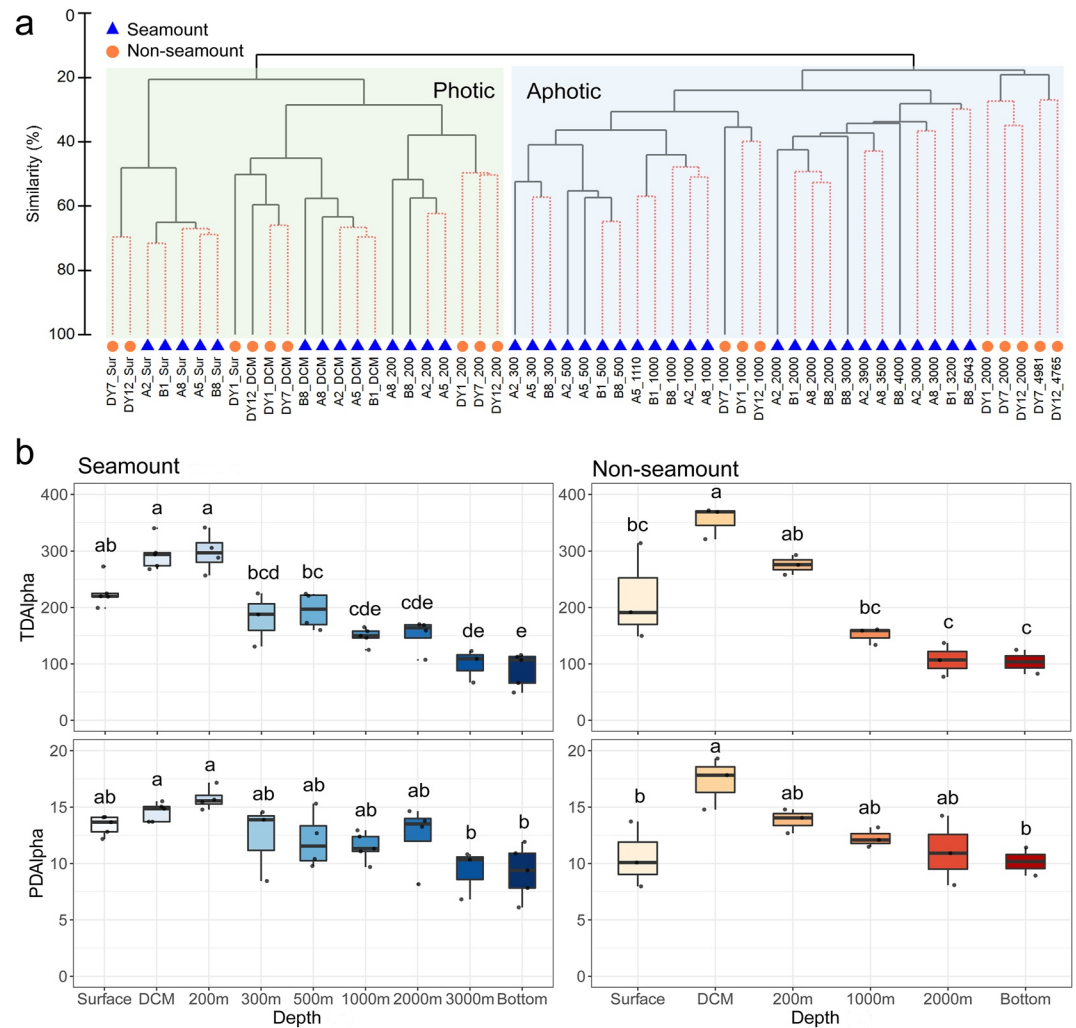


Figure 2. (a) Cluster plot based on the Bray-Curtis distance matrix of all samples. Red dotted line represents the adjoining samples have no significant difference according to SIMPROF analysis ($P > 0.05$). (b) TDAAlpha and PDAAlpha of ciliate communities along depth gradients in the seamount (left panel) and nonseamount areas (right panel). The groups of Fisher-LSD test were annotated in the plot.

waters increased. Over half of karyorelicteans in the 2,000 m layer came from the 3,000 m (19%) or bottom (35%) water layers, and 67% of karyorelicteans in the 3,000 m layer came from the bottom water.

3.2. Quantification of Selection, Dispersal, and Drift Structuring Pelagic Communities

The ciliate communities in the seamount and nonseamount areas were both primarily determined by variable selection with the explanations of 48.08% and 40.44%, respectively, followed by the homogeneous dispersal with the respective contributions of 35.56% and 30.88%. The homogeneous selection barely contributed to the community variations. Dispersal limitation and drift took more importance in the nonseamount area than in the seamount (Figure 4a).

3.3. Effects of Environmental Selection on Ciliate Community

Depth exerted strong and significant direct influence on the TDAAlpha and PDAAlpha of ciliate community in the nonseamount area, while the direct influence of depth was subtle and no significant effect was observed in the seamount area (Figure 4b). The ENV block (temperature, salinity, and DO) significantly influenced the TDAAlpha of ciliate communities in both the seamount and nonseamount areas, while it was insignificant for the PDAAlpha.

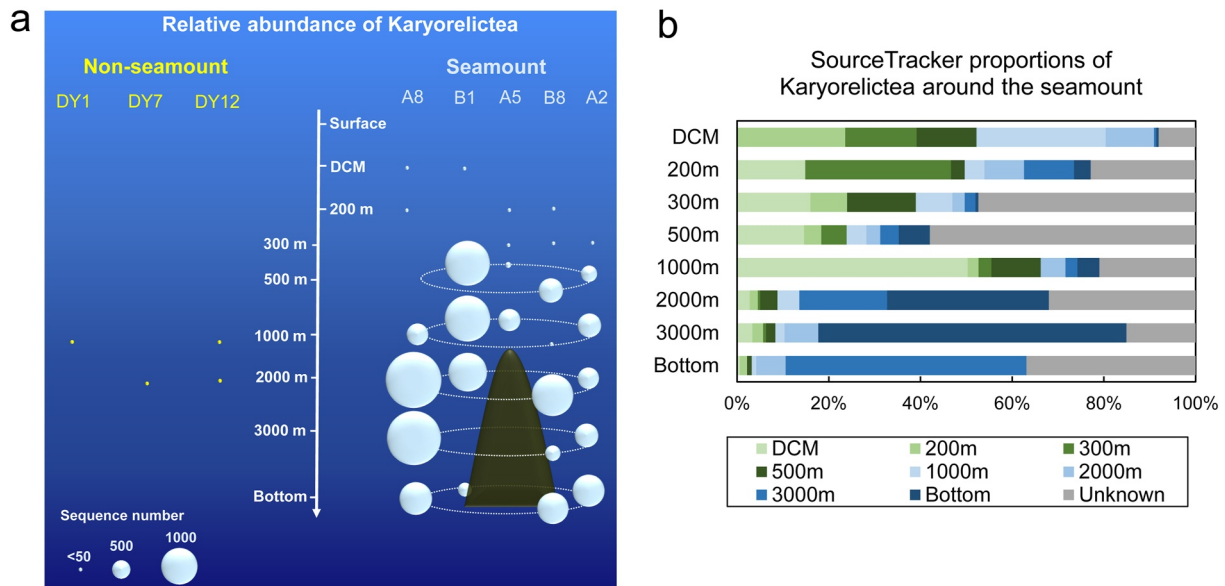


Figure 3. (a) Relative abundance of the bottom-dwelling Karyorelictea in different water layers in the seamount and nonseamount areas. The size of each solid circle is in proportion to the sequence number of Karyorelictea. (b) SourceTracker proportions of different water layers estimated for Karyorelictea around the seamount.

The TDA α and PDA α of ciliate community were better explained in the nonseamount area with the R^2 values of 0.87 and 0.63, respectively, compared with those of the seamount ciliate community ($R^2 = 0.686$ and 0.376, respectively).

The pure effect of DEPTH, NUTR, ENV, and BIO appeared to be significant on ciliate community from both the seamount and nonseamount areas with varying proportions (Figure 4c). In the seamount ciliate community, the ENV took the greatest proportions both in explanations of the TDBeta (9.1%) and PDBeta (4.5%), and the BIO (Chl a) occupied the least contributions to the TDBeta and PDBeta. In the nonseamount area, the DEPTH and NUTR ($\text{NO}_3\text{-N}$, $\text{NO}_2\text{-N}$, $\text{NH}_4\text{-N}$, $\text{PO}_4\text{-P}$, $\text{SiO}_3\text{-Si}$, TN, and TP) took the greatest proportions for TDBeta and PDBeta. The independent explained variations of depth were generally lower in the seamount (1.4% for TDBeta, 0.9% for PDBeta) than those in the nonseamount area (10.7% for TDBeta, 1.7% for PDBeta; Figure 4c). The total contributions of depth to the TDBeta and PDBeta around the seamount were also lower than those in the nonseamount area.

3.4. Dispersal Processes Influencing Ciliate Community Connectivity

Samples in the nonseamount area only significantly related to those in the same water layer (Figure 5a). Around the seamount, the surface and DCM samples only correlated with samples from the same depth, while samples below 300 m presented significant correlations with samples from different water layers. Modularity indexes of sample-sample network in the seamount and nonseamount areas were 0.651 and 0.613, respectively, while the average clustering coefficients were 0.699 and 0.889 in the seamount and nonseamount areas, respectively.

The proportions of shared ZOTUs of samples from the same station in the seamount and nonseamount areas were respectively calculated. Along the vertical profile, the mean proportion of shared ZOTUs in the seamount samples from the same station was higher than that in the nonseamount samples, particularly in samples at and below 2,000 m (Table S5 in Supporting Information S1).

3.5. Physical Drivers for Ciliate Community Connectivity

Many mesoscale eddies, which could be found by satellite altimetry and by reanalysis models, occurred in the Kocebu Guyot area (Figure S3 in Supporting Information S1). The mesoscale eddies are frequent in this region, associated with strong upward flows; for example, strong upward flows frequently occurred with a maximum velocity up to 1×10^{-5} m/s (~ 0.8 m/day) and could sustain for several months (Figure S4 in Supporting Information S1). As a result, the study area is characterized with mean upward flows, as indicated by the long-term mean upward vertical velocity above the seamount (Figure 6). At the seamount stations A5, A8, and A2, the mean upward flows with magnitude of 0.5×10^{-5} m/s (~ 0.4 m/day) could extend from the summit to ~ 200 m; at stations

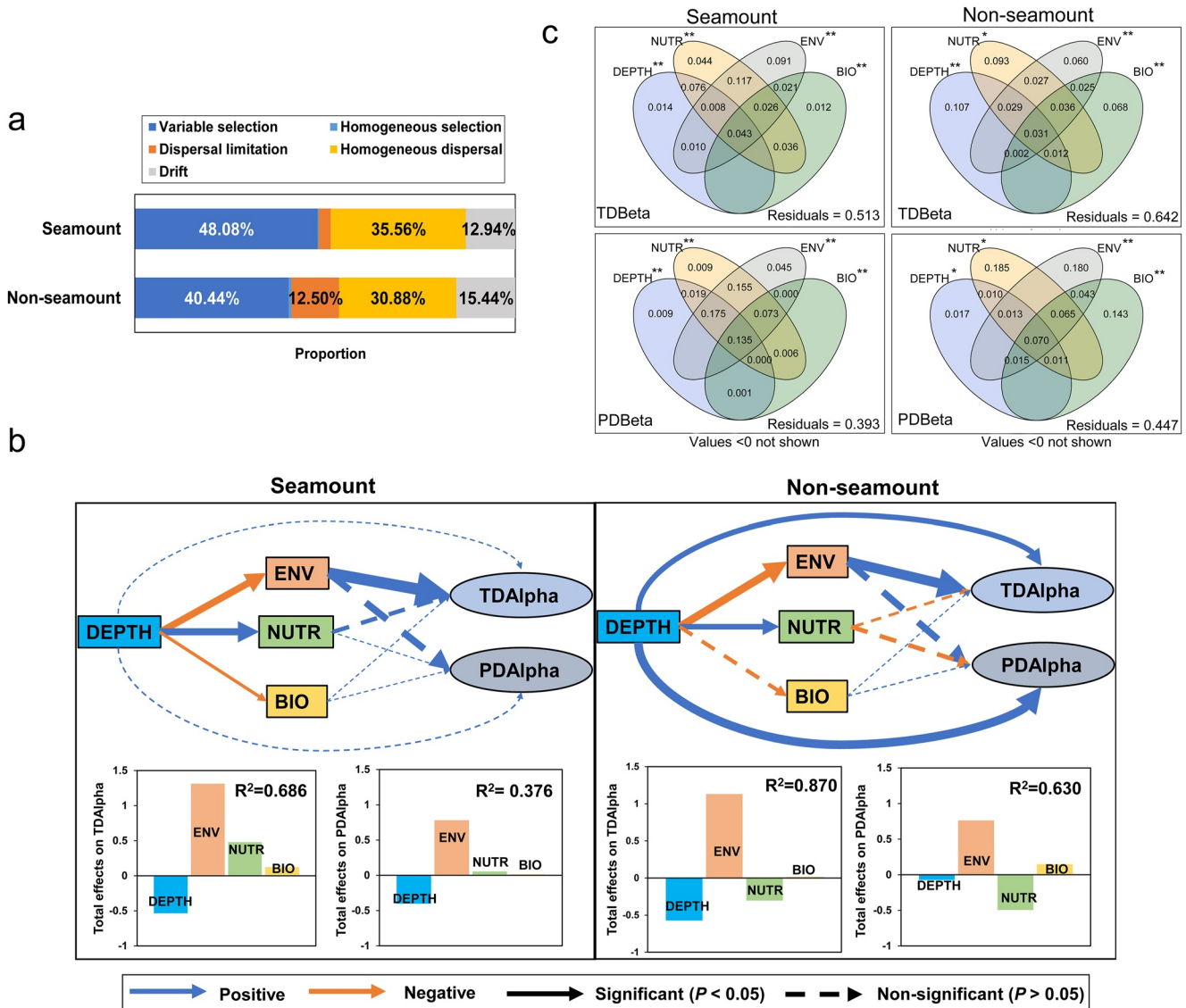


Figure 4. (a) Relative proportions of ecological processes shaping ciliate communities in the seamount and nonseamount areas. (b) The direct effects of environmental factors on taxonomic (TDA α) and phylogenetic (PDA α) alpha diversity based on the final partial least squares path models (PLS-PM). The width of arrows indicates the influential degree of each block. The lower barplots show the total effects of each latent variable. (c) The effects of environmental factors on the taxonomic (TDBeta) and phylogenetic (PDBeta) beta diversity based on the VPA. Individual variances and significant levels of ANOVA permutation tests are annotated in corresponding parts (* $P < 0.05$ and ** $P < 0.01$).

B1 and B8, there were also mean upward flows with similar magnitude between 200 and 1,000 m (Figures 6a, 6c, and 6d). On the contrary, the upward flow was very weak at depths from 200 to 1,000 m in the nonseamount area like station DY7, and the long-time mean vertical velocity was about 1 order lower than that around the seamount. The mean upward flows in the study area are crucial for the maintenance of the bottom dwellers in the upper layers.

3.6. Taxon–Taxon Cooccurrence Relationships

After ZOTUs filtration using the same standard, the cooccurrence relationship of the seamount ciliates (Figure 5b) consisted of 84 nodes and 348 edges with the average degree or node connectivity of 8.286, while the cooccurrence relationship in the nonseamount area consisted of 67 nodes and 215 edges with the average degree of 6.418. The modularity index of the seamount and nonseamount networks was 0.719 and 0.826, respectively. Negative correlations took a higher percentage of 20.47% in the nonseamount area than those of 16.95% around the seamount. The core taxa around the seamount were the classes Spirotrichea, Karyorelictea, and Nassophorea, while those in the nonseamount area were Spirotrichea, Nassophorea, and Oligohymenophorea.

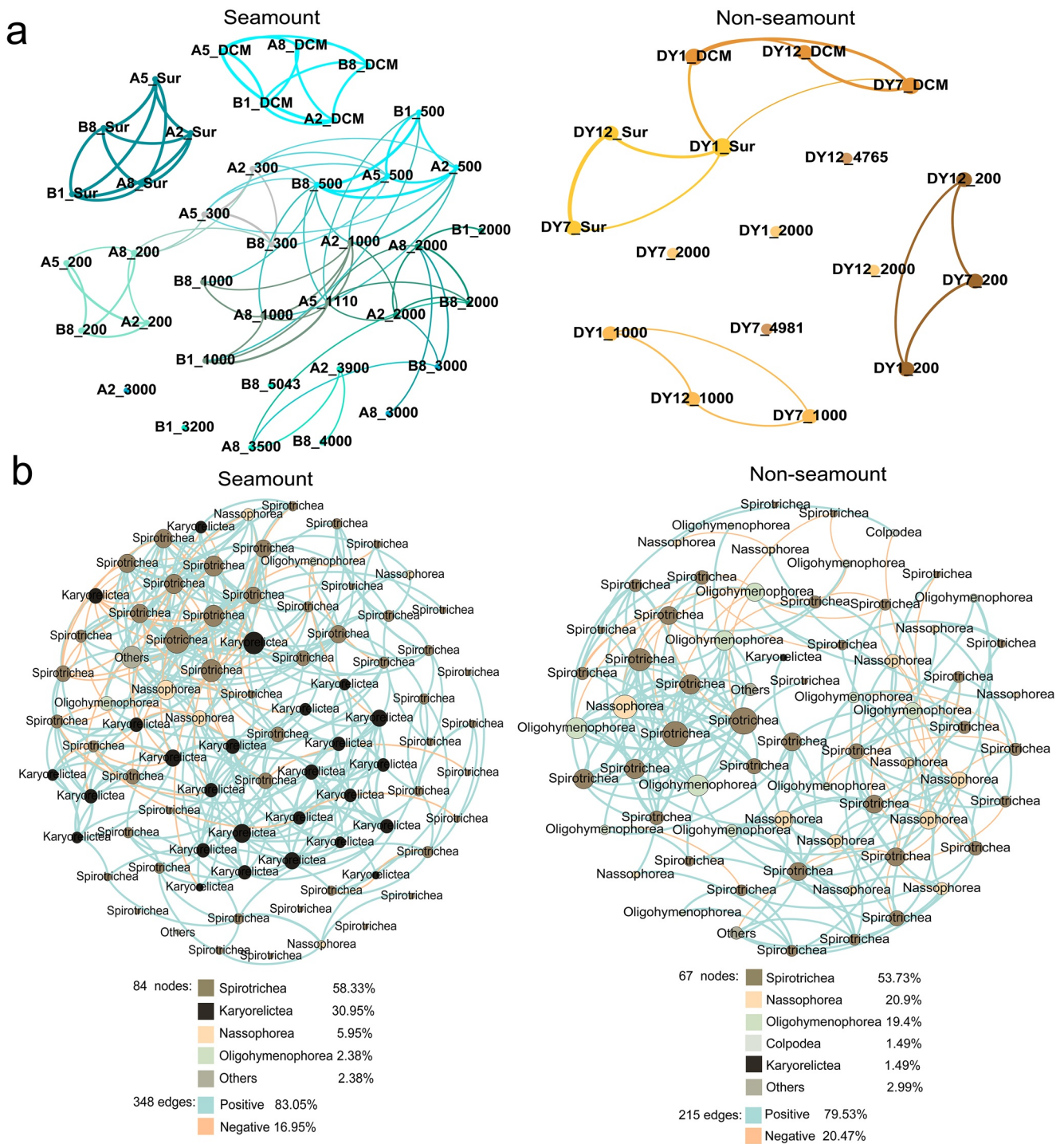


Figure 5. (a) Sample–sample networks indicating significant Spearman’s correlations of samples in the seamount and nonseamount areas. The nodes represent samples from different water layers. Edges represent significant correlations. (b) Taxon–taxon network illustrating the cooccurrence relationships of ciliate groups. The nodes represent zero-radius operational taxonomic units (ZOTUs) with annotation of assigned class. Blue edges represent positive correlations and orange edges represent negative ones.

The taxon–taxon relationship at each station along the water column around the seamount contained a much higher number of nodes and edges compared with that in the nonseamount area (Figures S5 and S6 in Supporting Information S1). In the seamount area, the mean value of average path length was 2.665, and that of modularity index was 0.896 for each separate network. In the nonseamount area, the mean value of average path length was

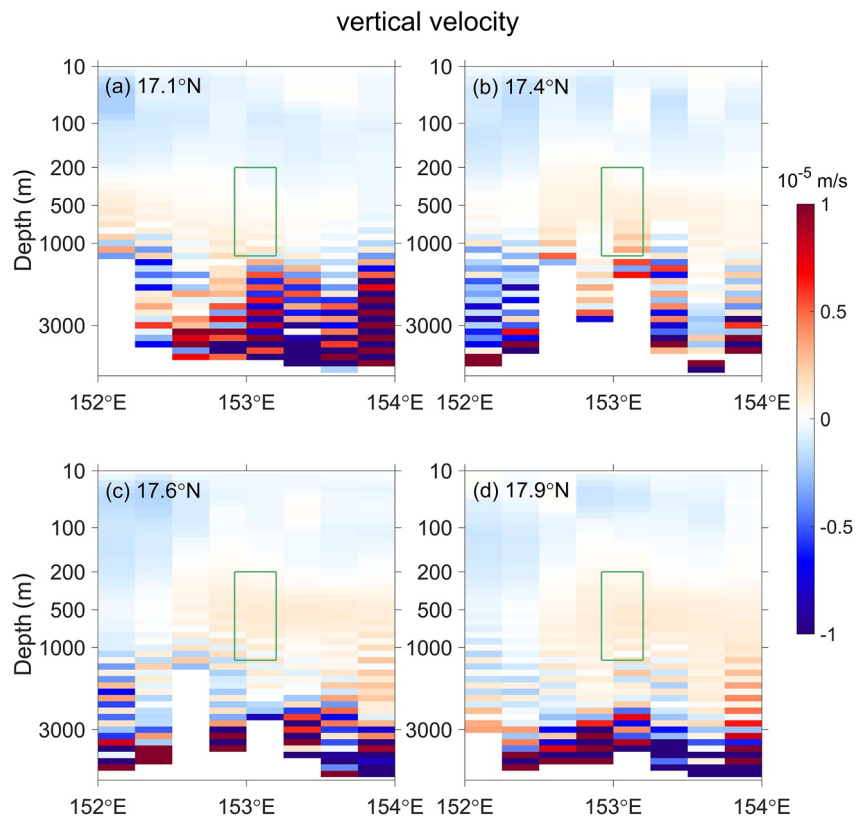


Figure 6. Five-year (2009–2013) mean vertical velocity (in m/s) at: (a) 17.1°N, (b) 17.4°N, (c) 17.6°N, and (d) 17.9°N based on the ECCO simulation. The green boxes denote the upward flow over the Kocebu Guyot latitudes.

3.538 and that of modularity index was 1.240 (Table S6 in Supporting Information S1). Karyorelicteans in the seamount area were present in taxon–taxon networks from the bottom water layer up to the 200 m layer and the proportion of Karyorelictea out of the total taxa in each network decreased roughly from the bottom to the 200 m layer (Figure S7 in Supporting Information S1).

4. Discussion

4.1. Evidence of Deep Seamount Effects

Deep seamounts, particularly those whose summits are deeper than 1,000 m, were previously thought to have limited impact on their surrounding environments. By investigating the ciliate communities around the Kocebu Guyot and those in a nonseamount area, we found that the deep seamount enhanced the vertical mixing and cooccurrence complexity of the ciliate community to an extent of over 1,000 m above the summit (Figure 7). The vertical mixing is composed of a strong uplift in the deep water and an upward weak uplift in the shallow water. The strong vertical mixing was shown by the presence of abundant bottom-dwelling Karyorelictea uplifted from the bottom water to the 500 m water layer, about 700 m above the summit (Figure 7). Karyorelicteans as typical microbenthos have been found mainly in marine interstitial habitats (Foissner, 1998), and they are also frequently found in sediments from a seamount about 2,000 km from the Kocebu Guyot (Zhao, Filker, Xu, et al., 2017). Like the distinct uplift of bottom dwellers, Ma et al. (2020a) observed an uplift of temperature and concentration of particulate organic carbon around the Kocebu Guyot, which reached to about 450 m above the summit (−1,198 m). A similar uplift was also shown by observation of a deep anticyclonic cap about 600 m above the summit (−1,308 m) around the nearby deep seamount Caiwei Guyot (Guo et al., 2020).

Furthermore, the ciliate community provides a higher-resolution record of the deep seamount effects, which uplifted the bottom-dwellers karyorelicteans to the DCM (about 150 m) water layer (Figure 7). A similar uplift signal was confirmed by the upward transport of nutrients and enhanced phytoplankton observed on the Kocebu Guyot (Dai et al., 2022), while a recent study of bacteria, protists, and fungi around the Kocebu Guyot held

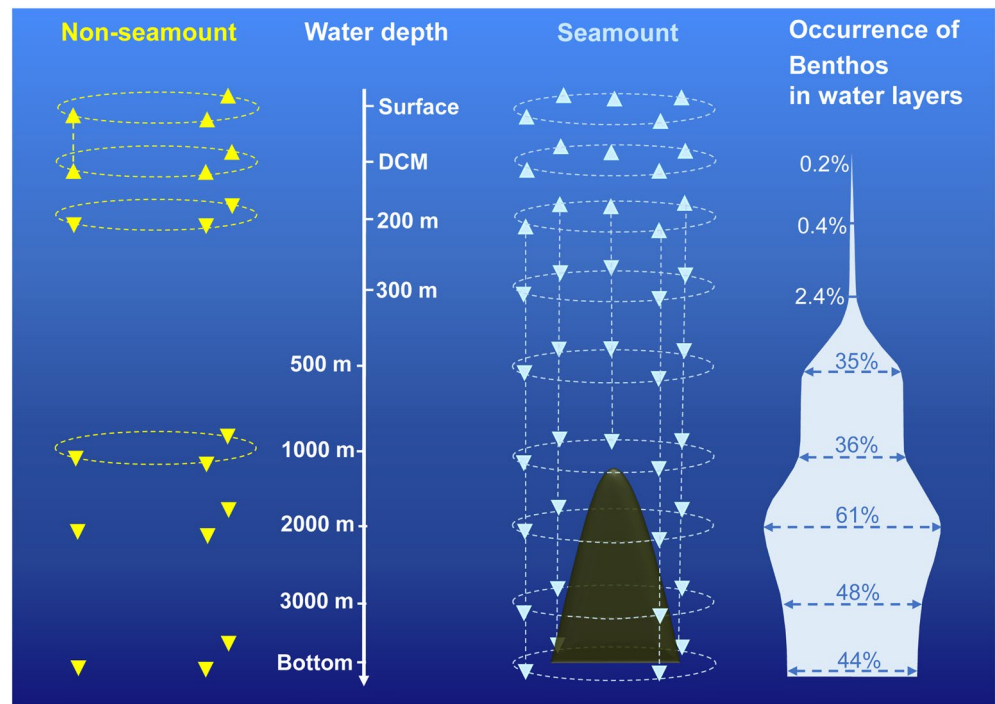


Figure 7. The conceptual model of horizontal and vertical connectivity patterns of ciliate communities in the seamount and nonseamount areas. The solid triangles represent samples, with upward and downward directions indicating the two major groups of ciliate communities in each area. The dashed line connecting samples means significant cooccurrence relationships between samples. The right violin shows the proportion of benthic forms in the total ciliate community.

clues of deep seamount impact on the diversity and connectivity of pelagic communities, the vertical influential range was unclear (Zhao, Zhao, Zheng, et al., 2022). This study, together with the physico-chemical and biological indications, suggests the existence of deep seamount effects that enhances the vertical mixing and promotes the connectivity of aphotic and photic waters. Considering the wide existences of deep seamounts worldwide, such an effect may have ecological significance and enhance the cycles of matter and energy of global oceans. Nonetheless, a deep seamount effect has been documented only in the tropical western Pacific Ocean, and whether such effect frequently occurs in the world ocean remains unknown.

4.2. Seamount Enhances Vertical Connectivity and Cooccurrence Complexity

According to the sample–sample cooccurrence networks, the ciliate communities around the seamount showed higher connectivity than those in the nonseamount area among all the water layers, and much higher connectivity occurred below the seamount summit. Furthermore, above the summit water layers, the mean proportion of shared ZOTUs among samples from the vertical profile of the same station had subtle difference from those in the nonseamount area. The vertically shared proportions around seamount below the summit water layers were significantly higher than those in the nonseamount area (Table S5 in Supporting Information S1). Moreover, seamount ciliates showed significant higher proportions of shared ZOTUs between DCM and 200 m as well as 1,000 and 2,000 m than that of nonseamount area (Table S7 in Supporting Information S1). These findings indicate a higher vertical connectivity of community around the deep seamount, which strongly expands previous understanding of seamount effects on planktons from shallow seamounts (Eriksen, 1998; Lueck & Mudge, 1997) and intermediate-depth ridge (Meredith et al., 2015).

We further revealed that the enhanced vertical connectivity could promote the taxon–taxon cooccurrence relationships, which were more complex in the seamount communities than the nonseamount ones. In our study, the bottom-dwellers Karyorelictea played a vital role in the taxon–taxon networks of ciliates and took about one third of the number of network nodes in the seamount area, while they hold an extremely low proportion in the nonseamount area. Our analysis indicated that Karyorelictea in the seamount upper water layers mainly came from the lower water layers, further supporting the effect of enhanced vertical mixing. Water depth is generally considered

a main factor limiting the distribution of both planktonic and benthic ciliates (Grattepanche et al., 2016; Sun et al., 2020; Zhao, Filker, Stoeck, et al., 2017). The seamount effects by enhancing the connectivity significantly promoted the vertical communication of different water layers, and thus redistributed the organisms. Different physico-chemical and trophic conditions of different water layers may boost the diversification of organisms.

4.3. Potential Hydrodynamic Processes Contribute to the Vertical Migration of Benthic Karyorelictea

We hypothesize that mesoscale oceanic eddies could be an important driving factor to the vertical migration of the benthic Karyorelictea via maintain overall constant upward flows. When an impinging flow encounters a seamount, an anticyclonic cap, which is composed of an anticyclonic circulation at the foot and a bottom trapped anticyclonic circulation over the summit, may be generated (Guo et al., 2020; Huppert & Bryan, 1976; Owens & Hogg, 1980). Simultaneously, a radial–vertical secondary circulation can be induced, which consists of downward flows above the summit center, offshore flows at the summit rim and up-slope flows above the rim (Guo et al., 2020). Due to abundant surface-intensified mesoscale eddies which may extend to over 1,000 m deep (Chelton et al., 2011) and subsurface-intensified mesoscale eddies which cover the depths of ~300 to more than 1,000 m (Feng et al., 2021; Xu et al., 2019) passing by the Magellan Seamount Chain, the current associated with eddies frequently results in upward flows which may last for several months.

During our survey, we encountered an anticyclonic surface-intensified eddy to the west of the seamount stations and a cyclonic surface-intensified eddy to the north of the stations, both of which had strong horizontal velocities extending from the surface to nearly the bottom (Figure S3a in Supporting Information S1). Despite differences in the manifestation of surface eddies between modeled and observed SLA (Figures S3a and S3b in Supporting Information S1), we still see similar patterns in the modeled SLA (Figure S3b in Supporting Information S1), associated with upward velocities ($\sim 3 \times 10^{-5}$ m/s, ~ 2.5 m/day) around the seamount (Figure S3c in Supporting Information S1). The upwelling should be responsible for the unusual presence of benthic Karyorelictea ciliates in the upper layers. In addition, we obtained a 5-year mean vertical upward flow caused by persistent eddy-induced upwellings (Figure S4 in Supporting Information S1), with a vertical velocity ~ 0.4 m/day (Figure 6). This suggests that this region is undergoing an overall upward flow, which is crucial for the maintenance of the bottom dwellers in the upper layers. Nonetheless, internal wave-induced vertical mixing could also be an option for the vertical transport of the benthic Karyorelictea near the submit of the seamount, since it is usually enhanced near the rough bottom (Ledwell et al., 2000); however, no evidence is available to prove that this kind of mixing can extend from 1,000 to 200 m depths.

5. Conclusions

The distribution pattern and connectivity of ciliate community were detected from a deep seamount and compared with those from a nonseamount area in the western Pacific Ocean. We presented a distinct deep seamount effect, which enhanced the vertical connectivity of planktonic communities to an uplift extent of 1,000 m above the summit. Such an effect was indicated by the presence of bottom dwellers in the water column and more complex cooccurrence relationships in the seamount community compared with that of nonseamount community. The increase in vertical exchange is attributed to the reduction of the influence of water depth on ciliate community by the seamount. This finding expands previous understanding of seamount effects originated from the shallow and intermediate-depth seamounts.

Conflict of Interest

The authors declare no conflicts of interest relevant to this study.

Data Availability Statement

Sequence data have been submitted to the Sequence Read Archive database under accession number PRJNA795881. The data link is <https://www.ncbi.nlm.nih.gov/bioproject/PRJNA795881> (Zhao, Zhao, Fang, et al., 2022).

Acknowledgments

The research was supported by the National Natural Science Foundation of China (Grants 41930533 and 41976099), the Strategic Priority Research Program of the Chinese Academy of Sciences (Grant XDB42000000), and the Youth Innovation Promotion Association CAS (Grant 2022206). We thank the crews of the *R/V KeXue* for their support in sample collection.

References

- Azam, F., Fenchel, T., Field, J. G., Gray, J. S., Meyerreil, L. A., & Thingstad, F. (1983). The ecological role of water-column microbes in the sea. *Marine Ecology Progress Series*, *10*(3), 257–263. <https://doi.org/10.3354/meps010257>
- Barberan, A., Bates, S. T., Casamayor, E. O., & Fierer, N. (2012). Using network analysis to explore co-occurrence patterns in soil microbial communities. *The ISME Journal*, *6*(2), 343–351. <https://doi.org/10.1038/ismej.2011.119>
- Cardoso, P., Rigal, F., & Carvalho, J. C. (2015). BAT—Biodiversity Assessment Tools, an R package for the measurement and estimation of alpha and beta taxon, phylogenetic and functional diversity. *Methods in Ecology and Evolution*, *6*(2), 232–236. <https://doi.org/10.1111/2041-210x.12310>
- Cavender-Bares, J., Kozak, K. H., Fine, P. V. A., & Kembel, S. W. (2009). The merging of community ecology and phylogenetic biology. *Ecology Letters*, *12*(7), 693–715. <https://doi.org/10.1111/j.1461-0248.2009.01314.x>
- Chapman, D. C., & Haidvogel, D. B. (1992). Formation of Taylor caps over a tall isolated seamount in a stratified ocean. *Geophysical & Astrophysical Fluid Dynamics*, *64*(1–4), 31–65. <https://doi.org/10.1080/03091929208228084>
- Chase, J. M., Kraft, N. J. B., Smith, K. G., Vellend, M., & Inouye, B. D. (2011). Using null models to disentangle variation in community dissimilarity from variation in alpha-diversity. *Ecosphere*, *2*(2), art24. <https://doi.org/10.1890/es10-00117.1>
- Chelton, D. B., Schlax, M. G., & Samelson, R. M. (2011). Global observations of nonlinear mesoscale eddies. *Progress in Oceanography*, *91*(2), 167–216. <https://doi.org/10.1016/j.pocean.2011.01.002>
- Clark, M. R., Rowden, A. A., Schlacher, T., Williams, A., Consalvey, M., Stocks, K. I., et al. (2010). The ecology of seamounts: Structure, function, and human impacts. *Annual Review of Marine Science*, *2*(1), 253–278. <https://doi.org/10.1146/annurev-marine-120308-081109>
- Dai, S., Zhao, Y., Li, X., Wang, Z., Zhu, M., Liang, J., et al. (2022). Seamount effect on phytoplankton biomass and community above a deep seamount in the tropical western Pacific. *Marine Pollution Bulletin*, *175*, 113354. <https://doi.org/10.1016/j.marpolbul.2022.113354>
- de Vargas, C., Audic, S., Henry, N., Decelle, J., Mahe, F., Logares, R., et al. (2015). Eukaryotic plankton diversity in the sunlit ocean. *Science*, *348*(6237), 1261605. <https://doi.org/10.1126/science.1261605>
- Dixon, P. (2003). VEGAN, a package of R functions for community ecology. *Journal of Vegetation Science*, *14*(6), 927–930. [https://doi.org/10.1658/1100-9233\(2003\)014\[0927:VAPORF\]2.0.CO;2](https://doi.org/10.1658/1100-9233(2003)014[0927:VAPORF]2.0.CO;2)
- Dolan, J. R., Claustre, H., Carlotti, F., Plounevez, S., & Moutin, T. (2002). Microzooplankton diversity: Relationships of tintinnid ciliates with resources, competitors and predators from the Atlantic Coast of Morocco to the Eastern Mediterranean. *Deep Sea Research Part I: Oceanographic Research Papers*, *49*(7), 1217–1232. [https://doi.org/10.1016/s0967-0637\(02\)00021-3](https://doi.org/10.1016/s0967-0637(02)00021-3)
- Edgar, R. C. (2013). UPARSE: Highly accurate OTU sequences from microbial amplicon reads. *Nature Methods*, *10*(10), 996–998. <https://doi.org/10.1038/nmeth.2604>
- Edgar, R. C. (2018). Updating the 97% identity threshold for 16S ribosomal RNA OTUs. *Bioinformatics*, *34*(14), 2371–2375. <https://doi.org/10.1093/bioinformatics/bty113>
- Edgar, R. C., & Flyvbjerg, H. (2015). Error filtering, pair assembly and error correction for next-generation sequencing reads. *Bioinformatics*, *31*(21), 3476–3482. <https://doi.org/10.1093/bioinformatics/btv401>
- Eriksen, C. C. (1998). Internal wave reflection and mixing at Fieberling Guyot. *Journal of Geophysical Research*, *103*(C2), 2977–2994. <https://doi.org/10.1029/97JC03205>
- Faith, D. P. (1992). Conservation evaluation and phylogenetic diversity. *Biological Conservation*, *61*(1), 1–10. [https://doi.org/10.1016/0006-3207\(92\)91201-3](https://doi.org/10.1016/0006-3207(92)91201-3)
- Fenchel, T. (1987). *Ecology of protozoa: The biology of free-living phagotrophic protists* (pp. 102–116). Springer. <https://doi.org/10.1007/978-3-662-06817-5>
- Feng, L., Liu, C., Köhl, A., Stammer, D., & Wang, F. (2021). Four types of baroclinic instability waves in the global oceans and the implications for the vertical structure of mesoscale eddies. *Journal of Geophysical Research: Oceans*, *126*, e2020JC016966. <https://doi.org/10.1029/2020JC016966>
- Foissner, W. (1998). The karyorelictids (Protozoa: Ciliophora), a unique and enigmatic assemblage of marine, interstitial ciliates: A review emphasizing ciliary patterns and evolution. In *Evolutionary Relationships Among Protozoa* (Vol. 56, pp. 305–325).
- Foissner, W. (2006). Biogeography and dispersal of micro-organisms: A review emphasizing protists. *Acta Protozoologica*, *45*(2), 111–136.
- Gao, X., Chen, H., Govaert, L., Wang, W., & Yang, J. (2019). Responses of zooplankton body size and community trophic structure to temperature change in a subtropical reservoir. *Ecology and Evolution*, *9*(22), 12544–12555. <https://doi.org/10.1002/ece3.5718>
- Genin, A. (2004). Bio-physical coupling in the formation of zooplankton and fish aggregations over abrupt topographies. *Journal of Marine Systems*, *50*(1–2), 3–20. <https://doi.org/10.1016/j.jmarsys.2003.10.008>
- Gimmler, A., Korn, R., de Vargas, C., Audic, S., & Stoeck, T. (2016). The Tara Oceans voyage reveals global diversity and distribution patterns of marine planktonic ciliates. *Scientific Reports*, *6*(1), 33555. <https://doi.org/10.1038/srep33555>
- Gordon, L., Jennings, J., Ross, A., & Krest, J. (1993). A suggested protocol for continuous flow automated analysis of seawater nutrients (phosphate, nitrate, nitrite and silicic acid) in the WOCE hydrographic program and the Joint Global Ocean Fluxes Study. In *Methods Manual WHPO*, 91-1.
- Gouy, M., Guindon, S., & Gascuel, O. (2010). SeaView version 4: A multiplatform graphical user interface for sequence alignment and phylogenetic tree building. *Molecular Biology and Evolution*, *27*(2), 221–224. <https://doi.org/10.1093/molbev/msp259>
- Graham, C. H., & Fine, P. V. A. (2008). Phylogenetic beta diversity: Linking ecological and evolutionary processes across space in time. *Ecology Letters*, *11*(12), 1265–1277. <https://doi.org/10.1111/j.1461-0248.2008.01256.x>
- Grattepainche, J.-D., Santoferrara, L. F., McManus, G. B., & Katzt, L. A. (2016). Unexpected biodiversity of ciliates in marine samples from below the photic zone. *Molecular Ecology*, *25*(16), 3987–4000. <https://doi.org/10.1111/mec.13745>
- Guillou, L., Bachar, D., Audic, S., Bass, D., Berney, C., Bittner, L., et al. (2013). The protist ribosomal reference database (PR2): A catalog of unicellular eukaryote small sub-unit rRNA sequences with curated taxonomy. *Nucleic Acids Research*, *41*(D1), D597–D604. <https://doi.org/10.1093/nar/gks1160>
- Guo, B., Wang, W., Shu, Y., He, G., Zhang, D., Deng, X., et al. (2020). Observed deep anticyclonic cap over Caiwei Guyot. *Journal of Geophysical Research: Oceans*, *125*, e2020JC016254. <https://doi.org/10.1029/2020jc016254>
- Heino, J., & Tolonen, K. T. (2017). Ecological drivers of multiple facets of beta diversity in a lentic macroinvertebrate metacommunity. *Limnology & Oceanography*, *62*(6), 2431–2444. <https://doi.org/10.1002/lno.10577>
- Huppert, H. E., & Bryan, K. (1976). Topographically generated eddies. *Deep Sea Research and Oceanographic Abstracts*, *23*(8), 655–679. [https://doi.org/10.1016/S0011-7471\(76\)80013-7](https://doi.org/10.1016/S0011-7471(76)80013-7)
- Jiang, Y., Yang, E. J., Kim, S. Y., Kim, Y.-N., & Lee, S. (2014). Spatial patterns in pelagic ciliate community responses to various habitats in the Amundsen Sea (Antarctica). *Progress in Oceanography*, *128*, 49–59. <https://doi.org/10.1016/j.pocean.2014.08.006>

- Kembel, S. W., Cowan, P. D., Helmus, M. R., Cornwell, W. K., Morlon, H., Ackerly, D. D., et al. (2010). Picante: R tools for integrating phylogenies and ecology. *Bioinformatics*, 26(11), 1463–1464. <https://doi.org/10.1093/bioinformatics/btq166>
- Knights, D., Kuczynski, J., Charlson, E. S., Zaneveld, J., Mozer, M. C., Collman, R. G., et al. (2011). Bayesian community-wide culture-independent microbial source tracking. *Nature Methods*, 8(9), 761–763. <https://doi.org/10.1038/nmeth.1650>
- Koslow, J. A., Boehlert, G. W., Gordon, J. D. M., Haedrich, R. L., Lorange, P., & Parin, N. (2000). Continental slope and deep-sea fisheries: Implications for a fragile ecosystem. *ICES Journal of Marine Science*, 57(3), 548–557. <https://doi.org/10.1006/jmsc.2000.0722>
- Lara, E., Berney, C., Harms, H., & Chatzinotas, A. (2007). Cultivation-independent analysis reveals a shift in ciliate 18S rRNA gene diversity in a polycyclic aromatic hydrocarbon-polluted soil. *FEMS Microbiology Ecology*, 62(3), 365–373. <https://doi.org/10.1111/j.1574-6941.2007.00387.x>
- Ledwell, J. R., Montgomery, E. T., Polzin, K. L., St Laurent, L. C., Schmitt, R. W., & Toole, J. M. (2000). Evidence for enhanced mixing over rough topography in the abyssal ocean. *Nature*, 403(6766), 179–182. <https://doi.org/10.1038/35003164>
- Lueck, R. G., & Mudge, T. D. (1997). Topographically induced mixing around a shallow seamount. *Science*, 276(5320), 1831–1833. <https://doi.org/10.1126/science.276.5320.1831>
- Ma, J., Song, J., Li, X., Yuan, H., Li, N., Duan, L., & Wang, Q. (2020a). Geochemical characteristics of particulate organic carbon in the Kocebu Seamount waters of the western Pacific Ocean in spring 2018. *Advances in Earth Science*, 35(7), 731–741. <https://doi.org/10.11867/j.issn.1001-8166.2020.057>
- Ma, J., Song, J. M., Li, X. G., Yuan, H. M., Li, N., Duan, L., & Wang, Q. D. (2020b). Control factors of DIC in the Y3 seamount waters of the western Pacific Ocean. *Journal of Oceanology and Limnology*, 38(4), 1215–1224. <https://doi.org/10.1007/s00343-020-9314-3>
- Marshall, J., Adcroft, A., Hill, C., Perelman, L., & Heisey, C. (1997). A finite-volume, incompressible Navier Stokes model for studies of the ocean on parallel computers. *Journal of Geophysical Research*, 102(C3), 5753–5766. <https://doi.org/10.1029/96jc02775>
- Mathieu, B., Sebastien, H., & Mathieu, J. (2009). Gephi: An open source software for exploring and manipulating networks. Paper presented at International AAAI Conference on Weblogs and Social Media. Association for the Advancement of Artificial Intelligence. <https://doi.org/10.13140/2.1.1341.1520>
- McArdle, B. H., & Anderson, M. J. (2001). Fitting multivariate models to community data: A comment on distance-based redundancy analysis. *Ecology*, 82(1), 290–297. [https://doi.org/10.1890/0012-9658\(2001\)082\[0290:FMMTCD\]2.0.CO;2](https://doi.org/10.1890/0012-9658(2001)082[0290:FMMTCD]2.0.CO;2)
- Menemenlis, D., Campin, J., Heimbach, P., Hill, C., Lee, T., Nguyen, A., et al. (2008). ECCO2: High resolution global ocean and sea ice data synthesis. *Mercator Ocean Quarterly Newsletter*, 31, 13–21.
- Meredith, M. P., Meijers, A. S., Garabato, A. C. N., Brown, P. J., Venables, H. J., Abrahamson, E. P., et al. (2015). Circulation, retention, and mixing of waters within the Weddell-Scotia Confluence, Southern Ocean: The role of stratified Taylor columns. *Journal of Geophysical Research: Oceans*, 120, 547–562. <https://doi.org/10.1002/2014JC010462>
- Mohn, C., White, M., Denda, A., Erofeeva, S., Springer, B., Turnewitsch, R., & Christiansen, B. (2021). Dynamics of currents and biological scattering layers around Senghor Seamount, a shallow seamount inside a tropical northeast Atlantic eddy corridor. *Deep Sea Research Part I: Oceanographic Research Papers*, 171, 103497. <https://doi.org/10.1016/j.dsr.2021.103497>
- Owens, W. B., & Hogg, N. G. (1980). Oceanic observations of stratified Taylor columns near a bump. *Deep Sea Research Part A: Oceanographic Research Papers*, 27(12), 1029–1045. [https://doi.org/10.1016/0198-0149\(80\)90063-1](https://doi.org/10.1016/0198-0149(80)90063-1)
- Parsons, T. R., Maita, Y., & Lalli, C. M. (1984). Fluorometric determination of chlorophylls. In *A manual of chemical & biological methods for seawater analysis* (pp. 107–109). Pergamon Press.
- Pierce, R. W., & Turner, J. T. (1992). Ecology of planktonic ciliates in marine food webs. *Reviews in Aquatic Sciences*, 6(2), 139–181.
- Price, M. N., Dehal, P. S., & Arkin, A. P. (2010). FastTree 2—approximately maximum-likelihood trees for large alignments. *PLoS One*, 5(3), e9490. <https://doi.org/10.1371/journal.pone.0009490>
- Read, J., & Pollard, R. (2017). An introduction to the physical oceanography of six seamounts in the southwest Indian Ocean. *Deep Sea Research Part II: Topical Studies in Oceanography*, 136, 44–58. <https://doi.org/10.1016/j.dsr2.2015.06.022>
- Rogers, A. D. (1994). The biology of seamounts. *Advances in Marine Biology*, 30, 305–350. [https://doi.org/10.1016/s0065-2881\(08\)60065-6](https://doi.org/10.1016/s0065-2881(08)60065-6)
- Rogers, A. D. (2018). The biology of seamounts: 25 Years on. *Advances in Marine Biology*, 79, 137–224. <https://doi.org/10.1016/bs.amb.2018.06.001>
- Sanchez, G. (2013a). *PLS path modeling with R*. Trowchez Editions.
- Sanchez, G. (2013b). PLSPM package. Retrieved from <https://github.com/gastonstat/plspm.git>
- Stegen, J. C., Lin, X., Fredrickson, J. K., Chen, X., Kennedy, D. W., Murray, C. J., et al. (2013). Quantifying community assembly processes and identifying features that impose them. *The ISME Journal*, 7(11), 2069–2079. <https://doi.org/10.1038/ismej.2013.93>
- Stegen, J. C., Lin, X., Fredrickson, J. K., & Konopka, A. E. (2015). Estimating and mapping ecological processes influencing microbial community assembly. *Frontiers in Microbiology*, 6, 370. <https://doi.org/10.3389/fmicb.2015.00370>
- Stock, A., Edgcomb, V., Orsi, W., Filker, S., Breiner, H.-W., Yakimov, M. M., & Stoeck, T. (2013). Evidence for isolated evolution of deep-sea ciliate communities through geological separation and environmental selection. *BMC Microbiology*, 13(1), 150. <https://doi.org/10.1186/1471-2180-13-150>
- Stocks, K. I., Clark, M. R., Rowden, A. A., Consalvey, M., & Schlacher, T. A. (2012). CenSeam, an international program on seamounts within the census of marine life: Achievements and lessons learned. *PLoS One*, 7(2), e32031. <https://doi.org/10.1371/journal.pone.0032031>
- Stoeck, T., Bass, D., Nebel, M., Christen, R., Jones, M. D. M., Breiner, H. W., & Richards, T. A. (2010). Multiple marker parallel tag environmental DNA sequencing reveals a highly complex eukaryotic community in marine anoxic water. *Molecular Ecology*, 19, 21–31. <https://doi.org/10.1111/j.1365-294X.2009.04480.x>
- Sun, P., Wang, Y., Laws, E., & Huang, B. (2020). Water mass-driven spatial effects and environmental heterogeneity shape microeukaryote biogeography in a subtropical, hydrographically complex ocean system—A case study of ciliates. *Science of the Total Environment*, 706, 135753. <https://doi.org/10.1016/j.scitotenv.2019.135753>
- Wickham, H. (2016). *ggplot2: Elegant graphics for data analysis*. Springer-Verlag.
- Xu, A., Yu, F., & Nan, F. (2019). Study of subsurface eddy properties in northwestern Pacific Ocean based on an eddy-resolving OGCM. *Ocean Dynamics*, 69(4), 463–474. <https://doi.org/10.1007/s10236-019-01255-5>
- Zhao, F., Filker, S., Stoeck, T., & Xu, K. D. (2017). Ciliate diversity and distribution patterns in the sediments of a seamount and adjacent abyssal plains in the tropical western Pacific Ocean. *BMC Microbiology*, 17(1), 192. <https://doi.org/10.1186/s12866-017-1103-6>
- Zhao, F., Filker, S., Xu, K. D., Huang, P. P., & Zheng, S. (2017). Patterns and drivers of vertical distribution of the ciliate community from the surface to the abyssopelagic zone in the western Pacific Ocean. *Frontiers in Microbiology*, 8, 2559. <https://doi.org/10.3389/fmicb.2017.02559>
- Zhao, R. J., Zhao, F., Feng, L., Fang, J. K.-H., Liu, C. Y., & Xu, K. D. (2022). Ciliate community in the Magellan Seamount [Dataset]. PRJNA. Retrieved from <https://dataview.ncbi.nlm.nih.gov/object/PRJNA795881>
- Zhao, R. J., Zhao, F., Zheng, S., Li, X. G., Wang, J. N., & Xu, K. D. (2022). Bacteria, protists, and fungi may hold clues of seamount impact on diversity and connectivity of deep-sea pelagic communities. *Frontiers in Microbiology*, 13, 773487. <https://doi.org/10.3389/fmicb.2022.773487>